Int. J. Heat Mass Transfer. Vol. 20, pp. 675–683. Pergamon Press 1977. Printed in Great Britain

AN INTEGRAL ENERGY-BALANCE MODEL FOR THE MELTING OF SOLIDS ON A HOT MOVING SURFACE, WITH APPLICATION TO THE TRANSPORT PROCESSES DURING EXTRUSION

OWEN M. GRIFFIN
Ocean Technology Division, Naval Research Laboratory, Washington, DC 20375, U.S.A.

(*Received* 7 *July* 1976 *and in revised form* 21 *September* 1976)

Abstract—This paper describes an energy-balance integral method for analyzing the contact melting of solids on a hot, moving surface. Temperature-dependent viscosity, sensible heat and viscous heat generation terms are included in the melting model, which is suitable in practice for inclusion in any of several proposed formulations for modeling the polymer melting processes in extruders. Two example cases are computed and compared with experimental data for the solid bed profile in an extruder. The first is one in which both viscous heat generation and temperature-dependent viscosity effects are important, while the second example is one in which the large temperature difference across the melt film is predominant and the viscous heat generation is relatively unimportant. Good agreement between the melting model and the experiments is obtained for both cases.

NOMENCLATURE

a_i, coefficient in the temperature profile defined by (7);
A, melt film Stefan number, $\bar{C}_{PF}(\bar{T}_W - \bar{T}_M)/\bar{M}$;
b, temperature coefficient of viscosity [°C^{-1}];
b', normalized temperature coefficient of viscosity defined by (9);
B, solid phase Stefan number, $\bar{C}_{PS}(\bar{T}_M - \bar{T}_O)/\bar{M}$;
Br, melt film Brinkman number, $\bar{\mu}_M \bar{V}_W^2/k_F(\bar{T}_W - \bar{T}_M)$;
$\bar{C}_P$, specific heat [J/kg°C];
D, generalized Stefan number defined by (14);
D_1, coefficient in the energy-balance integral formulation defined by (16a);
$\bar{h}, h$, film thickness [m]; normalized film thickness;
$\bar{h}_0$, clearance between the screw flight and extruder barrel [m];
I_1, I_2, I_3, integral functions defined by (9), (10) and (13);
$\bar{k}$, thermal conductivity [W/m °C];
L, length of the solid bed in the $\bar{x}$ direction [m];
L_0, width of screw channel normal to the screw flight [m];
$\dot{\bar{m}}, \dot{m}$, mass flow rate in the $\bar{x}$ direction [kg/s]; normalized mass flow rate;
$\dot{m}''$, melting rate of polymer defined by (20);
$\bar{M}$, latent heat of fusion [J/kg];
Pe, melt film Peclet number, $\bar{V}_W L/\bar{\alpha}_F$;
R_1, R_2, shielding ratios defined by (18), (19);
$\bar{T}, T$, temperature [°C]; normalized temperature;
$\bar{u}, u$, velocity in the $\bar{x}$ direction [m/s]; normalized velocity;
$\bar{v}, v$, velocity in the $\bar{y}$ direction [m/s]; normalized velocity;
$\bar{V}_W$, velocity of the heated surface [m/s];
$\bar{x}, x$, distance along the heated surface [m]; normalized distance;
$\bar{y}, y$, distance normal to the heated surface [m]; normalized distance;
$\bar{z}, z$, distance along the screw channel [m]; normalized distance.

Greek symbols

$\bar{\alpha}$, thermal diffusivity [m^2/s];
ε, packing fraction of the granular polymer;
η, normalized distance defined by (7);
$\bar{\mu}, \mu$, melt viscosity [Ns/m^2]; normalized viscosity;
$\bar{\rho}$, density [kg/m^3];
$\bar{\tau}, \tau$, shear stress in the melt [N/m^2]; normalized shear stress.

Subscripts

F, melt film;
M, interfacial boundary between melt and solid phases;
O, extruder barrel;
S, solid phase;
W, heated wall.

1. INTRODUCTION

THERE are many important and practical engineering systems in which heat and mass transfer are accompanied by melting or freezing. The large temperature gradients which exist in the melting sections of extruders and on melting grids produce conditions where the phase transformation is combined with temperature-dependent property variations, viscous heat generation and sensible heat effects that must be appropriately taken into account. A completely satisfactory method for the design of single-screw plasticating extruders depends on the existence of a suitable mathematical model for the polymer melting process, and optimal design methods are presently not available. The need for increased efficiency and energy savings

in processing make the continuing study of melting models desirable.

A survey of the state-of-the-art as regards melting models for extruders recently was published by Shapiro and Pearson [1] in connection with the development of a more precise physical description for the phase transformation process. Also, Pearson [2] has presented a study of the governing equations for the melting of beds of granular polymers and has included an ordering of terms and the development of similarity parameters for the system of equations. The equations and similarity variables obtained by Pearson are the same as those obtained some time ago by Young [3] in a related study. Young's work on contact melting was an outgrowth of the classical studies of Ross [4] for grids and of Tadmor and Klein [5] for screw extruders.

A series of elegant modeling experiments by Vermeulen [6] and Vermeulen, Scargo and Beek [7] yielded a significant body of experimental data for grid melting and for the melting section of an extruder. Vermeulen also suggested a simple pure-conduction, constant-property model for the melting section of an extruder. Griffin [8], employing an energy-balance integral formulation, included convection, variable property and variable melt layer thickness terms in the melting model and provided a preliminary, but positive, comparison with Vermeulen's experimental results. The same energy-balance integral method had previously been applied successfully to the case of contact melting on grids [9, 10].

The purpose of the present paper is to describe in more detail an energy-balance integral model for the melting processes in an extruder. Temperature-dependent viscosity, sensible heat and viscous heat generation terms are included in the melting model and a general solution taking account of these effects is obtained in a relatively simple and straightforward manner. Some comparisons are made between measured data and an analytical model for the solid bed profile in the melting section of an extruder.

2. THEORETICAL DEVELOPMENT OF THE MELTING MODEL

The energy-balance integral analysis was developed by Goodman [11] for the analysis of transient, one-dimensional heat conduction problems with melting or freezing at a system boundary. Motion of the fluid must be taken account of in many practical systems and Goodman's original method has been extended to these more recently [8–10]. One typical example of a complex heat-transfer system with phase change is the melting section of a plasticating extruder.

The system considered here is shown in Fig. 1 which outlines the idealization of an extruder section normal to the screw flight. The ordering of the terms in the governing equations for such a system has been carried out by Pearson [2] and Young [3], and the resulting governing equations, in normalized form, are:

$$\text{Continuity:} \quad \frac{\partial u}{\partial x}+\frac{\partial(v\xi)}{\partial y}=0, \tag{1}$$

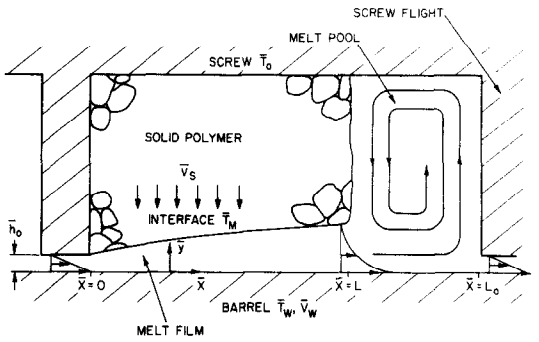

FIG. 1. Melting on a hot, moving surface as in an idealized cross-section of an extruder. The plane of the figure is normal to the screw flight; in the coordinates illustrated the barrel is moving and the screw is stationary as assumed in practice, c.f. [5].

$$\text{Momentum:} \quad \frac{\partial \tau}{\partial y}=\frac{\partial}{\partial y}\left(-\mu(T)\frac{\partial u}{\partial y}\right)=0, \tag{2}$$

$$\text{Energy:} \quad u\frac{\partial T}{\partial x}+v\xi\frac{\partial T}{\partial y}=\frac{1}{Pe}\frac{\partial^2 T}{\partial y^2}-\frac{Br}{Pe}\tau\frac{\partial u}{\partial y}. \tag{3}$$

Here viscous heat generation, temperature-dependent viscosity and convection terms are included, and the motion in the melt film is approximated by purely drag flow [2, 3, 6]. It sometimes is necessary to include shear-rate viscosity dependence, but the features of the melting model can be amply demonstrated by the Newtonian form of equation (2) which is valid for crystalline polymers.

An energy balance at the interface leads to the equation

$$\left(-\frac{\partial T}{\partial y}\right)_{y=h^-}=\frac{Pe}{A}\frac{\mathrm{d}\dot{m}}{\mathrm{d}x}+\frac{\bar{k}_s(\bar{T}_M-\bar{T}_O)}{\bar{k}_F(\bar{T}_W-\bar{T}_M)}\left(-\frac{\partial T_s}{\partial y}\right)_{y=h^+} \tag{4}$$

and after the heat conduction into the solid is evaluated by assuming one-dimensional conduction in a moving medium, equation (4) reduces to

$$\left(-\frac{\partial T}{\partial y}\right)_{y=h}=\left(\frac{1+B}{A}\right)\xi Pe, \quad \xi=\frac{\mathrm{d}\dot{m}}{\mathrm{d}x}. \tag{4a}$$

Here A and B are the Stefan numbers for the melt and solid, respectively. These equations are related to the physical system in Fig. 1 by the transformation

$$x=\frac{\bar{x}}{L}, \quad y=\frac{\bar{y}}{L}, \quad u=\frac{\bar{u}}{\bar{V}_W}, \quad v=\frac{\bar{v}}{\bar{v}_F}, \quad \xi=\frac{\bar{v}_F}{\bar{V}_W}$$

$$T=\frac{\bar{T}-\bar{T}_M}{\bar{T}_W-\bar{T}_M}, \quad T_S=\frac{\bar{T}-\bar{T}_O}{T_M-T_O}, \quad \dot{m}=\frac{\dot{\bar{m}}}{\bar{\rho}_F\bar{V}_W L}$$

$$Pe=\frac{\bar{V}_W L}{\bar{\alpha}_F}, \quad Br=\frac{V_W^2\mu_M}{\bar{k}_F(\bar{T}_W-\bar{T}_M)}$$

$$A=\frac{\bar{C}_{PF}(\bar{T}_W-\bar{T}_M)}{\bar{M}}, \quad B=\frac{\bar{C}_{PS}(\bar{T}_M-\bar{T}_O)}{\bar{M}}.$$

The boundary conditions, again in normalized form, are

$$\begin{aligned} &y=0: \quad u=1, \ v=0, \ T=1, \\ &y=h: \quad u\approx 0, \ v=-1, \ T=0. \end{aligned} \tag{5}$$

where the melt velocity at $y = h$ is derived from an interfacial mass balance

$$\bar{v}_F = \frac{\bar{\rho}_S}{\rho_F}\bar{v}_S \tag{6}$$

when the x components of the interfacial velocities and the solid bed velocity are neglected. It should be noted here that the interfacial velocities $\bar{v}_F$ and $\bar{v}_S$ in general are functions of the distance $\bar{x}$ along the heated surface. Thus the normalized melting rate ξ in the governing equations (1), (3) and (4a) is also a function of x and is an unknown quantity in the problem at the outset.

It has been shown [8–10] that a cubic temperature profile best simulates the actual temperature distribution in a variety of polymer melting problems. Let the temperature therefore be specified by

$$T(x, y) = \sum_{j=0}^{3} a_j \eta^j, \quad \eta = \frac{y}{h} \tag{7}$$

where the a_j are to be obtained from specified constraints and where h is the local and, as yet, unknown melt film thickness. The momentum equation can be solved directly. The shear stress is assumed to be of the form

$$\tau = \frac{\bar{\tau}L}{\bar{\mu}_M V_W} = -\mu(T)\frac{\partial u}{\partial y} = -e^{-b(T-T_M)}\frac{\partial u}{\partial y} \tag{8}$$

and when substituted in equation (2) results in

$$\frac{\partial}{\partial y}\left(e^{-b'T}\frac{\partial u}{\partial y}\right) = 0, \quad b' = b(\bar{T}_W - \bar{T}_M),$$

where b' is a nondimensional parameter which yields a measure of the temperature dependence of the melt relative to the temperature difference across the film. After integrating twice and applying the boundary conditions, the solution to this equation is

$$u(\eta) = 1 - \frac{1}{I_1}\int_0^\eta e^{b'T}\,d\eta, \quad I_1 = \int_0^1 e^{b'T}\,d\eta \tag{9}$$

where the temperature profile T is dependent on the normalized thickness η. The mass flux at any x is

$$\dot{m}(x) = \int_0^h u\,dy = h\int_0^1 u\,d\eta = hI_2, \quad x > 0 \tag{10}$$

and I_2 becomes, after substituting equation (9),

$$I_2 = 1 - \frac{1}{I_1}\int_0^1\left[\int_0^\eta e^{b'T}\,d\eta\right]d\eta. \tag{11}$$

The energy equation (3), when integrated with respect to y, reduces to

$$\left(-\frac{1}{Pe}\frac{\partial T}{\partial y}\right)_{y=0} + \frac{Br}{Pe}\tau = \left(-\frac{1}{Pe}\frac{\partial T}{\partial y}\right)_{y=h} + \frac{d}{dx}\int_0^h uT\,dy \tag{12}$$

since τ, from equation (2), is a function only of x. When the shear stress τ is evaluated from equation (8), and the energy equation is combined with the mass balance, equation (10), and the interfacial energy balance, equation (4a), the result is

$$\left[\int_0^1\left(-\frac{\partial T}{\partial \eta}\right)_{\eta=0}dx\right] + \frac{Br}{I_1} = \left[\int_0^1\left(\frac{\partial T}{\partial \eta}\right)_{\eta=1}dx\right]\left(1 + \frac{A}{1+B}T_B\right). \tag{12a}$$

Here the fluid bulk, or "cup mixing", temperature is given by

$$T_B = \frac{I_3}{I_2}, \quad I_3 = \int_0^1 uT\,d\eta. \tag{13}$$

The temperature distribution in the melt film is obtained by means of the energy-balance integral method. When the thermal boundary conditions, equation (5), are satisfied the temperature profile, equation (7), reduces to

$$T = 1 - \eta - a_2(\eta - \eta^2) - a_3(\eta - \eta^3). \tag{7a}$$

Two additional conditions are required in order to specify the coefficients a_2 and a_3. The first condition is obtained by taking the appropriate derivatives of equation (7a) and substituting in equation (12a), whereupon the integrated energy equation reduces to

$$(1 + a_2 + a_3) + Br/I_1 = (1 - a_2 - 2a_3)(1 + DT_B). \tag{14}$$

Here, for convenience, the Stefan numbers A and B for the melt and solid phases are combined into a single "generalized" Stefan number

$$D = \frac{A}{1+B}.$$

Following the usual procedures employed in the development of the energy-balance integral model [8, 11], the following conditions are used to specify the unknown functions a_2 and a_3:

(i) The boundary conditions (5) on the melt velocities at the interface;
(ii) The energy balance (4) at the interface;
(iii) The energy equation (3) evaluated at the interface.

These conditions reduce the energy equation at $y = h(\eta = 1)$ to

$$D\left(-\frac{\partial T}{\partial \eta}\right)^2_{\eta=1} = \left(\frac{\partial^2 T}{\partial \eta^2}\right)_{\eta=1} + \frac{Br}{I_1^2} \tag{15}$$

where again the Stefan numbers A and B are combined into the "generalized" Stefan number D. Substitution of the assumed temperature profile in equation (15) and solution of the resulting quadratic equation yields

$$a_3 = 0.5\{[(1-a_2)+1.5D] - \{[(1-a_2)+1.5D]^2 - [(1-a_2)^2 - D_1]\}^{1/2}\}, \tag{16}$$

where

$$D_1 = D\left[\frac{Br}{I_1^2} + 2a_2\right], \tag{16a}$$

and where the negative sign of the quantity under the square root symbol is chosen in order to satisfy compatibility requirements at the interface. The two energy-balance integral equations (14) and (16) completely

specify the unknown temperature profile. The temperature in the melt film is a function of the prominent non-dimensional parameters that govern the melting process, namely the Brinkman number Br, the Stefan numbers A and B and the temperature-dependence parameter of the viscosity b'.

The thickness variation of the melt film in the x-direction is obtained by integrating equations (4a), (7) and (10) after once establishing the temperature profile coefficients a_2 and a_3 in terms of the governing parameters just mentioned. The result is

$$h^2 = h_0^2 + \frac{2(1-a_2-2a_3)Ax}{PeI_2(1+B)}, \quad 0 \leqslant x \leqslant 1. \quad (17)$$

In this equation the initial condition is taken as the clearance h_0 between the screw flight and the barrel; this is a reasonable approximation as demonstrated by Vermeulen *et al.* [7] and Shapiro *et al.* [12], among others. Equation (17) for the melt film thickness is of the same form previously reported [8] for melting in the absence of viscous heat generation. Pearson [2] obtained the same result by means of dimensional analysis and a similarity transformation, though he did not solve the resulting set of governing equations.

A useful parameter in contact melting problems such as this is the shielding ratio R_1 or, in this case, the ratio of the heat transfer at the interface and the sum of the heat transfer at the moving surface plus the heat generation in the melt film. For the system considered in Fig. 1

$$R_1 = \frac{\int_0^L \left(-\bar{k}_F \frac{\partial \bar{T}}{\partial \bar{y}}\right)_{\bar{y}=\bar{h}} d\bar{x}}{\int_0^L \left(-\bar{k}_F \frac{\partial \bar{T}}{\partial \bar{y}}\right)_{\bar{y}=0} d\bar{x} - \int_0^L \int_0^{\bar{h}} \bar{\tau} \frac{\partial \bar{u}}{\partial \bar{y}} d\bar{y} d\bar{x}}, \quad (18)$$

or, in dimensionless terms,

$$R_1 = \frac{1}{1+DT_B}. \quad (18a)$$

The equation (18a) is derived from the overall energy balance which is employed together with equation (15) to specify the coefficients a_2 and a_3. A similar function by which to assess the influence of viscous heat generation in relation to the total heat transferred into and generated within the system is

$$R_2 = \frac{-\int_0^L \int_0^{\bar{h}} \bar{\tau} \frac{\partial \bar{u}}{\partial \bar{y}} d\bar{y} d\bar{x}}{\int_0^L \left(-\bar{k}_F \frac{\partial \bar{T}}{\partial \bar{y}}\right)_{\bar{y}=0} dx - \int_0^L \int_0^{\bar{h}} \bar{\tau} \frac{\partial \bar{u}}{\partial \bar{y}} d\bar{y} d\bar{x}}. \quad (19)$$

This ratio reduces to

$$R_2 = \frac{Br/I_1}{(1+a_2+a_3)+Br/I_1} \quad (19a)$$

in dimensionless terms. As will be demonstrated, the parameters R_1 and R_2 are very useful in estimating the relative contributions of the various heat-transfer mechanisms to the melting process.

3. HEAT-TRANSFER RESULTS FROM THE MELTING MODEL

Some representative heat-transfer results, utilizing the method just described, are given in Figs. 2–4. In all of the computations the properties of low-density

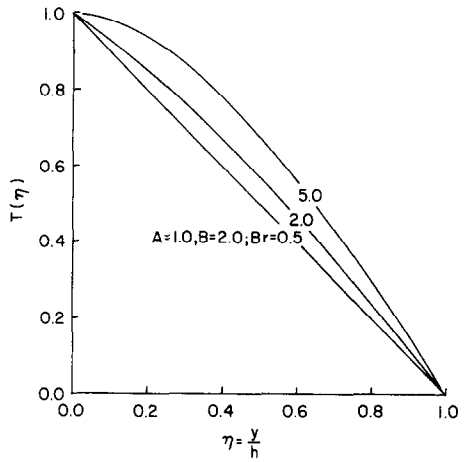

FIG. 2. The temperature distribution in the melt film as a function of the Brinkman number Br, for fixed values of the Stefan numbers A and B for the melt and solid phases.

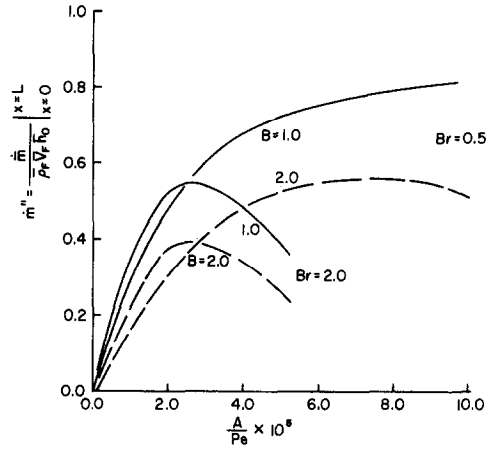

FIG. 3. The normalized melt rate, equation (20), as a function of the ratio A/Pe of the Stefan and Peclet numbers for the melt, for fixed values of the Brinkman number Br and the Stefan number B for the solid.

polyethylene (LDPE) were assumed, since that particular polymer is characterized by a well-defined melting point and highly temperature-dependent viscosity, i.e. $\mu_M = 4770\,\text{Ns/m}^2$, $b = 0.035°\text{C}^{-1}$ and $\bar{T}_M = 105°\text{C}$ [6].

The temperature profile, equation (7a), is plotted in Fig. 2 for three values of Brinkman number and for typical values of the Stefan numbers A and B. The condition $A = 1$ corresponds to a temperature difference $\bar{T}_W - \bar{T}_M = 43°\text{C}$ across the melt film, and $B = 2$ for the solid is likewise representative of the extrusion experiments reported by Vermeulen *et al.* [7]. The influence of viscous dissipation in the melt film is easily perceived from the results plotted in Fig. 2 and listed in Table 1. At the lowest value of Brinkman number, $Br = 0.5$, little effect of viscous heat generation appears

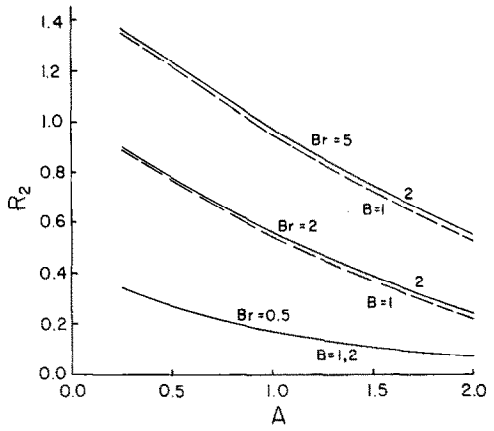

FIG. 4. The ratio R_2 of the viscous heat generation and the sum of viscous heat generation and conduction at the hot, moving surface as a function of the melt Stefan number A, for fixed values of the Brinkman number Br and the Stefan number B for the solid.

in the nearly linear temperature profile. In this case, about 75% of the energy added to the melt is conducted across the moving heated surface and 25% is generated by viscous forces. Of this total, about 80% is conducted across the melt interface and 20% is convected away by the melt film, as found from the shielding ratios R_1 and R_2. As the Brinkman number is increased to $Br = 2$ and still further to 5, the viscous heat generation portions of the energy input to the melt increase to 55% and to 95%, respectively. This increasing influence of the frictional heating also is evident from the increasingly convex form of the temperature profiles in Fig. 2 and from the increasing magnitude of the quadratic coefficient a_2 in the temperature profile (see Table 1).

Table 1. The effect of viscous dissipation on the temperature profile, $T = 1-\eta-a_2(\eta-\eta^2)-a_3(\eta-\eta^3)$ (Stefan numbers $A = 1.0$, $B = 2.0$)

Brinkman number, Br	a_2	a_3
0.5	−0.10	+0.067
2.0	−0.59	+0.21
5.0	−1.44	+0.49

The melting rate of polymer along the heated wall is conveniently expressed by the equation

$$\dot{m}'' = \frac{\dot{\bar{m}}}{\bar{\rho}_F \bar{V}_W \bar{h}_O}\Bigg|_{\bar{x}=0}^{\bar{x}=L}$$

$$= I_2\left\{1+\frac{2(1-a_2-2a_3)A}{h_O^2 I_2(1+B)Pe}\left(\frac{L}{L_O}\right)\right\}^{1/2} - 0.5 \quad (20)$$

where the length L_O normal to the screw flight is the characteristic length used to scale h_O and Pe. The melt rate $\dot{m}''$ is equal to the total melt flux at $\bar{x} = L$ less the melt carried across the screw flight at $x = 0$. Equation (20) again accounts for viscous heat generation, convection and variable-property effects on the melting rate. This equation is plotted in Fig. 3 for a range of Stefan numbers equal to $A = 0.25$–2 for the melt and $B = 1$ and 2 for the solid. Results for two Brinkman numbers ($Br = 0.5$ and 2) for the melt are shown and it should be noted that at constant Brinkman number the velocity of the heated wall $\bar{V}_W \approx (\bar{T}_W - \bar{T}_M)^{1/2}$. The range of nondimensional parameters and the length L/L_O of the solid bed in Fig. 3 are typical of extruder operating conditions as shown, for example, in Figs. 5 and 6.

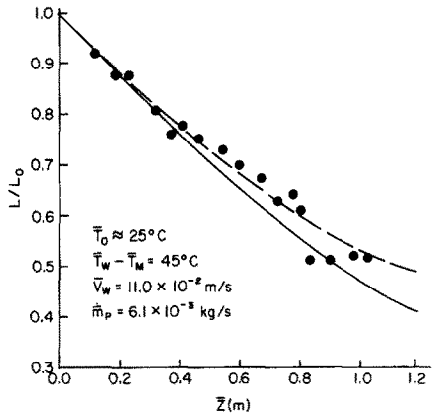

FIG. 5. The width of the solid bed L/L_0 in the melting section of an extruder as a function of the displacement $\bar{z}$ along the screw flight. $Br = 4.3$, $A = 1.0$, $B = 2.2$. Experimental data and properties for low-density polyethylene from [6]. Constant-property, pure conduction solution, [7] ——; equation (22) – – – –.

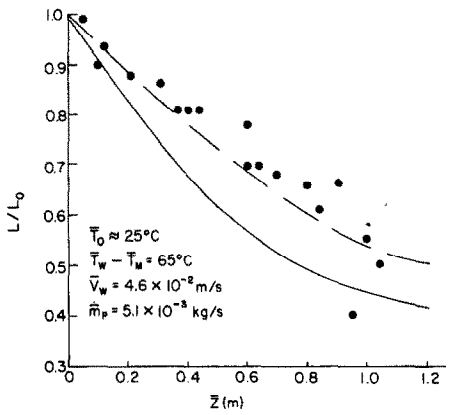

FIG. 6. The width of the solid bed L/L_0 in the melting section of an extruder as a function of the displacement $\bar{z}$ along the screw flight. $Br = 0.5$, $A = 1.5$, $B = 2.2$. Experimental data and properties for low-density polyethylene from [6]. Constant-property, pure conduction solution, [7] ——; equation (22) – – – –.

The melt rate dependence on the temperature difference across the melt film is clearly shown in the figure, with larger thermal gradients across the melt film resulting in a correspondingly increasing melt rate for $A < 1.5$. For Stefan numbers greater than this value the variable viscosity effects in the film predominate and the melt rate $\dot{m}''$ reaches a maximum and decreases

as the temperature difference across the film is increased still further. The actual melt rate $\dot{m}$ is proportional to $\bar{V}_W$ and increases very slowly or even decreases when $A > 1.5$. The Stefan number B for the solid also influences the melting rate; when the subcooling $(\bar{T}_M - \bar{T}_O)$ of the solid increases, the melting rate $\dot{m}''$ adjusts downward as shown in the figure owing to the increased conduction through the solid phase.

The importance of the temperature dependence of the viscosity to the melt flow behavior can be seen from the integrals I_1 and I_2 listed in Table 2. As seen from a comparison with the constant-property reference values, the temperature difference across the melt film has an important effect of the momentum equation (2). The integral I_1, which is a direct measure of the viscosity–temperature dependence and which is equal to unity in the constant-property case, increases by a factor of approximately six as the Stefan number of the melt increases from 0.25 to 2. The integral I_2, which is equal to one-half in the constant-property case, decreases from 0.47 to 0.28 over the Stefan number range just mentioned. It is also important to note that the integral I_2 is virtually independent of both the Brinkman number and the subcooling of the solid bed (denoted by the Stefan number B) and that I_1 is independent of B and only weakly dependent on the Brinkman number over an order of magnitude change in the latter. The influence of heat generation on the melting rate is primarily due to the coefficients a_2 and a_3 (which are both dependent on I_1) in the temperature gradient at the interface and to the relation

$$\bar{V}_W = [Br\bar{k}_F(T_W - T_M)/\bar{\mu}_M]^{1/2}$$

between the velocity (Peclet number) and the temperature difference across the melt film at constant Brinkman number.

The parameter R_2 of equation (19a), which is the ratio of the viscous heat generation term and the sum of heat generation and conduction at the heated wall, is plotted in Fig. 4. From these results it is possible to assess the importance of viscous heating of the melt over typical ranges of the Stefan and Brinkman numbers for both phases. At small Brinkman numbers the heat generation is important over the lowest segment of the melt Stefan number regime; for example, at $A = 0.5$, the heat generation is 37% of the heat conducted into the melt at $y = 0$ while at $A = 1.5$ and 2 respectively the heat generation in the melt is only 12% and 8% of the conduction term at the moving surface.

When the Brinkman number is increased to a large value such as $Br = 5$, the viscous heat generation becomes an important and often the predominat consideration. At large Stefan numbers such as $A = 2$, the heat generation term is 1.2 times the heat conducted into the melt at the moving heated wall. The effect of the heat generation becomes progressively greater until, at $A = 0.95$, the heat conduction at the heated wall falls to zero. Further evidence of this can be seen in Fig. 2 where the temperature gradient at $y = 0$ and for $Br = 5$ appears to be nearly zero. When the Stefan number is decreased still further at $Br = 5$, the direction of the heat conduction at the wall is changed. For $A = 0.75$, the viscous heat generation is predominant and is eleven times the heat conducted *away* from the melt at the moving surface. As with the integral functions I_1 and I_2 listed in Table 2, the results in Fig. 4 show that the ratio R_2 is strongly dependent on changes in the Brinkman number and the Stefan number (temperature difference) for the melt film, but is insensitive to changes in the subcooling of the solid phase for typical values of the Stefan number B. The results just described agree with the assertion by Lindt [13] that viscous heat generation may often be the predominant factor in the melting of polymers during extrusion.

Table 2. Temperature-dependence effects on flow in the melt film

Stefan number A	Stefan number B	Brinkman number Br	I_1 (Equation 9)	I_2 (Equation 11)
0.25	1.0*	0.5	1.23	0.467
0.5			1.51	0.438
1.0			2.30	0.378
2.0			5.81	0.272
0.25	1.0	5.0	1.28	0.468
0.5			1.60	0.438
1.0			2.49	0.380
2.0			6.31	0.278
(Constant-property solution, $b = 0$)			1.0	0.5

*Changes in B only slightly influence I_1 and have no influence on I_2.

4. APPLICATION OF THE MELTING MODEL

The energy-balance integral is applicable in practice for determining a variety of system parameters, including the solid bed profile in the melting section of an extruder. As an example, the computation of the solid bed profile in an extruder of constant channel cross-section is now considered. This simple geometry is sufficient to demonstrate the applicability of the melting model and its extension to more complicated

systems, which include a variable channel cross-section or a heated screw, is straightforward. These systems have been studied to varying degrees of complexity by Shapiro and Pearson [1], Lindt [13] and Donovan [14], among others.

The present model is derived from that of Vermeulen, Scargo and Beek [7]. In the latter case no account was taken of viscous heat generation, temperature-dependent viscosity and convection, and all are included here. It is assumed that changes in the $\bar{z}$ direction take place slowly and that the melting model described in the previous sections is valid locally at varying displacements along the screw channel. This is a common assumption in all extruder modeling studies. In addition, assuming a constant mass throughput rate $\dot{\bar{m}}_p$ in the direction $\bar{z}$ along the screw channel, the differential equation for the solid bed length L is

$$\left(\frac{\dot{\bar{m}}_p}{\bar{\rho}_F \bar{V}_W \bar{h}_O L_O I_2}\right)\frac{\mathrm{d}\left(\frac{L}{L_O}\right)}{\mathrm{d}z} = \frac{1}{2I_2} - \left[1 + \frac{2(1-a_2-2a_3)A\varepsilon}{PeI_2 h_O^2(1+B)}\left(\frac{L}{L_O}\right)\right]^{1/2}. \quad (21)$$

Here ε is the density ratio for the granular polymer relative to bulk solid.* For the experiments described by Vermeulen *et al.*, $\varepsilon = 0.65$. In this equation the Peclet number $Pe = \bar{V}_W L_O/\bar{\alpha}_F$, $z = \bar{z}/L_O$ and $h_O = \bar{h}_O/L$. When equation (21) is integrated with the initial condition $L = L_O$ at $\bar{z} = 0$, the solution is

$$(X+1)^{1/2} - \left(X\frac{L}{L_O}+1\right)^{1/2} + \frac{1}{2I_2}\ln\left[\frac{(X+1)^{1/2} - \frac{1}{2I_2}}{\left(X\frac{L}{L_O}+1\right)^{1/2} - \frac{1}{2I_2}}\right] = Yz \quad (22a)$$

where

$$X = \frac{2(1-a_2-2a_3)A\varepsilon}{PeI_2 h_O^2(1+B)}, \quad (22b)$$

$$Y = \tfrac{1}{2}\left(\frac{\bar{\rho}_F \bar{V}_W \bar{h}_O L_O I_2}{\dot{\bar{m}}_p}\right)X. \quad (22c)$$

*The melting rate $\dot{\bar{m}}$ of the solid polymer in equation (4) is multiplied by the factor ε in the case of the granular polymer. The film thickness h is then altered as shown in equation (21).

Two examples utilizing equation (22) are now considered. The experimental data were obtained by Vermeulen *et al.* [7] in an experimental study of the melting of low-density polyethylene, and the relevant extruder parameters and physical properties are tabulated in [6, 7]. In the first example shown in Fig. 5 the rotational speed and barrel temperature combine to result in a large Brinkman number and moderate Stefan number for the melt, c.f. Table 3(a). The screw was cooled during the experiments reported by Vermeulen *et al.* and this precluded any melting at the base of the screw. Thus the large Stefan number, $B = 2.2$, is a result of this cooling, i.e. large $(\bar{T}_M - \bar{T}_O)$. As a result of the large Brinkman number, $Br = 4.3$, about 87% of the energy addition to the melt is estimated to be a result of viscous heat generation and 13% to be from conduction at the barrel surface. Of this total energy added to the melt, about 80% is conducted across the melt interface and 20% is convected away by the melt flow. The integrals I_1 and I_2 corresponding to the conditions of Fig. 5 also suggest a significant departure from the constant-property case, as can also be seen from a comparison of the coefficients X and Y for the two cases in Table 3(a). The modified solid bed profile, equation (22), yields somewhat better agreement with the experimental data in Fig. 5 than does the constant-property, pure-conduction profile. The tendency of the constant-property solution to overestimate the melting rate at large values of $(\bar{T}_W - \bar{T}_M)$, and to correspondingly underestimate the solid bed profile, is offset in this case by the viscous heat generation term which is included in the present analysis but excluded from the constant-property, pure-conduction model.

Table 3. A comparison of the coefficients X and Y in the solid bed profile, equation (22)

(a)	$Br = 4.3$	$A = 1.0$	$B = 2.2$	$I_1 = 2.8$	$I_2 = 0.38$	(Fig. 5)
				Constant properties, pure conduction in film [7]	Equation (22)	
	X			1.19	2.97	
	$Y \times 10^2$			4.26	8.51	
(b)	$Br = 0.5$	$A = 1.5$	$B = 2.2$	$I_1 = 3.7$	$I_2 = 0.32$	(Fig. 6)
	X			4.38	7.80	
	$Y \times 10^2$			8.31	9.55	

The second example plotted in Fig. 6 and listed in Table 3(b) differs from the previous one in that the Brinkman number, $Br = 0.5$, is relatively small. Consequently the viscous heat generation contribution makes up only 15% of the energy added to the melt while 85% of the total energy input is conducted across the hot barrel surface. The temperature-dependence of the viscosity is more pronounced at this higher Stefan number $A = 1.5$, and the integral functions I_1 and I_2 again deviate substantially from the corresponding constant-property values owing to the relatively large temperature difference $(\bar{T}_W - \bar{T}_M = 65°C)$ across the melt film. The importance of taking the temperature-dependence of the viscosity into

account is illustrated once again by the much improved agreement between equation (22) and the experimental data in Fig. 6 as compared to the constant-property solution. The viscosity of the melt increases from 500 to 4700 Ns/m^2 across the melt film under the conditions plotted in Fig. 6, and the melt rate is considerably overestimated when the temperature-dependence of the melt viscosity is neglected.

5. SUMMARY AND CONCLUDING REMARKS

An energy-balance integral method for analyzing the contact melting of solids at a hot moving surface has been described. The method is suitable in practice for inclusion in any of several formulations for modeling the polymer melting processes in a screw extruder. Temperature-dependent viscosity, sensible heat and viscous heat generation terms are of general importance to this problem and can be included in the integral formulation in a relatively simple and straightforward manner. Several integral functions have been determined which allow one to estimate the relative contributions of the several heat-transfer mechanisms to the melting processes. The melting process is strongly dependent on the Brinkman number which characterizes the viscous heat generation and on the Stefan number for the melt which characterizes the ratio of sensible and latent heats for the film. At the large Stefan numbers which are typical of extrusion processes, the temperature-dependence of the viscosity has a limiting effect on the maximum melting rate which can be achieved. The large Brinkman numbers which are typical of polymer extrusion suggest that viscous heat generation often has a predominant effect on the melting process.

The integral melting model has been incorporated in a typical but relatively simple model for predicting the solid bed profile in an extruder of constant cross-section. This simple geometry is sufficient to demonstrate the applicability and the salient features of the integral model. Good agreement with experiment has been obtained in two example cases. The first concerns a system in which both viscous heat generation and temperature-dependent viscosity are important, and the second is one in which the large temperature difference across the melt film is the predominating factor and the viscous heat generation contribution is relatively small.

Acknowledgement—The author wishes to thank the Naval Research Laboratory for the support of this work.

REFERENCES

1. J. Shapiro and J. R. A. Pearson, A dynamic model for melting in plasticating extruders, Imperial College of Science and Technology, Polymer Science and Engineering Report No. 5 (1974).
2. J. R. A. Pearson, On the melting of solids near a hot moving interface, with particular reference to beds of granular polymers, *Int. J. Heat Mass Transfer* **19**, 405–411 (1976).
3. C. C. Young, The melting rate of highly crystalline polymers under shear conditions, Ph.D. Thesis, University of Connecticut (1970); see also *Poly. Engng Sci.* **12**, 59–63 (1972).
4. T. K. Ross, Heat transfer to fusible solids, *Chem. Engng Sci.* **1**, 212–215 (1952).
5. Z. Tadmor and I. Klein, *Engineering Principles of Plasticating Extrusion*, chapters 3 and 5. Van Nostrand-Reinhold, New York (1970).
6. J. R. Vermeulen, Het smelten van polymeerkorrels aan hete oppervlakken, Ph.D. Thesis, Technische Hogeschool Delft (1970).
7. J. R. Vermeulen, P. G. Scargo and W. J. Beek, The melting of crystalline polymers in a screw extruder, *Chem. Engng Sci.* **26**, 1457–1465 (1971).
8. O. M. Griffin, An integral method of solution for combined heat and mass transfer problems with phase transformation, *Heat Transfer 1974*, Vol. 1, pp. 211–215. Science Council of Japan, Tokyo (1974).
9. O. M. Griffin, On the melting of solids to non-Newtonian fluids, *Chem. Engng Sci.* **25**, 109–117 (1970).
10. O. M. Griffin, Heat transfer to molten polymers, *Poly. Engng Sci.* **12**, 140–149 (1972).
11. T. R. Goodman, The heat-balance integral and its application to problems involving change of phase, *Trans. Am. Soc. Mech. Engrs* **80**, 335–342 (1958).
12. J. Shapiro, A. L. Halmos and J. R. A. Pearson, Melting in single screw extruders: Parts 1 and 2, *Polymer* **17**, 905–918 (1976).
13. J. T. Lindt, A dynamic melting model for a single screw extruder, *Poly. Engng Sci.* **16**, 284–291 (1976).
14. R. C. Donovan, A theoretical melting model for plasticating extruders, *Poly. Engng Sci.* **11**, 247–257 (1971).

MODELE INTEGRAL DE BILAN ENERGETIQUE APPLICABLE A LA FUSION DE SOLIDES SUR UNE SURFACE CHAUDE EN MOUVEMENT, AVEC APPLICATION AUX PROCESSUS DE TRANSPORT LORS DE L'EXTRUSION

Résumé—L'article décrit une méthode intégrale de bilan énergétique pour l'étude de la fusion de solides au contact d'une surface chaude en mouvement. On a introduit, dans le modèle de fusion une viscosité dépendant de la température des termes sources de production de chaleur et la dissipation visqueuse, ce qui est en pratique approprié à l'introduction dans une des formulations proposées pour la modélisation des processus de fusion des polymères par extrusion. A titre d'exemple, deux cas sont calculés et comparés aux données expérimentales relatives aux profils de lit solide dans un dispositif d'extrusion. Dans le premier exemple la production de chaleur par dissipation visqueuse et les effets de variation de la viscosité avec la température sont tous deux importants, tandis que dans le deuxième exemple de grands écarts de température à travers le film en fusion sont déterminants et la production par dissipation visqueuse est relativement peu importante. On obtient dans les deux cas un bon accord entre le modèle de fusion et les expériences.

EIN ENERGIE-BILANZ-INTEGRAL-MODELL FÜR DAS SCHMELZEN VON FESTKÖRPERN AUF EINER HEISSEN, BEWEGTEN OBERFLÄCHE UND DIE ANWENDUNG AUF TRANSPORTVORGÄNGE IN EXTRUDERN

Zusammenfassung—Die Arbeit beschreibt eine Energiebilanz-Integral-Technik zur Beschreibung des Kontaktschmelzens von Festkörpern auf einer heißen, bewegten Oberfläche. Das Schmelzmodell berücksichtigt die Temperaturabhängigkeit der Viskosität und der spezifischen Wärmekapazität sowie die Wärmeerzeugung infolge Reibung; das Modell eignet sich in der Praxis zum Einsetzen in jede der vorgeschlagenen Formulierungen zur Beschreibung des Polymer-Schmelzvorganges in Extrudern. Es werden 2 Beispiele durchgerechnet und mit experimentellen Daten für die Festkörperprofile in Extrudern verglichen. Im ersten Fall spielen sowohl die Wärmeerzeugung infolge Reibung wie die Temperaturabhängigkeit der Viskosität eine Rolle, während im zweiten Fall große Temperaturdifferenzen im Schmelzgebiet dominieren und die Wärmeerzeugung infolge Reibung relativ unbedeutend ist. In beiden Fällen ergibt sich eine gute Übereinstimmung zwischen dem Schmelzmodell und den Versuchsergebnissen.

ИНТЕГРАЛЬНАЯ МОДЕЛЬ БАЛАНСА ЭНЕРГИИ ДЛЯ ОПИСАНИЯ ПРОЦЕССА ПЛАВЛЕНИЯ ТВЕРДЫХ ТЕЛ НА ГОРЯЧЕЙ ДВИЖУЩЕЙСЯ ПОВЕРХНОСТИ В ПРИМЕНЕНИИ К ПРОЦЕССАМ ПЕРЕНОСА ПРИ ЭКСТРУЗИИ

Аннотация — Интегральный метод баланса энергии используется для исследования контактного плавления твердых тел на горячей движущейся поверхности. Предложенная модель плавления учитывает зависимость вязкости от температуры, теплосодержание и теплоту вязкой диссипации; её удобно использовать на практике в любой из предложенных в работе формулировок для моделирования процессов плавления полимеров в экструдерах. В качестве примера рассчитаны два случая и дано сравнение с экспериментальными данными для профиля твердого слоя в экструдере. В первом случае доминирующими являются теплота вязкой диссипации и зависимость вязкости от температуры, в то время как во втором — значительная разность температур поперек расплава при несущественном влиянии вязкой диссипации. В обоих случаях получено хорошее соответствие теоретических результатов с данными экспериментов.